

LARGE LEWIS NO. EDGE-FLAME INSTABILITIES

J. Buckmaster

University of Illinois at Urbana-Champaign

INTRODUCTION

Edge-flames play an important role in a number of microgravity investigations, and in the general study of flames. Examples include the candle-flame experiments carried out on board both the Space-Shuttle and the Mir Space Station, e.g.[1]; the flame-spread-over-liquid work carried out by H.Ross and W.Sirignano, amongst others, e.g. [2,3]; and lifted turbulent diffusion flames. In all of these configurations a local two-dimensional flame structure can be identified which looks like a flame-sheet with an edge, and these structures exhibit dynamical behavior which characterizes them and distinguishes them from *ad hoc* 2D flame structures.

Edge-flames can exist in both a non-premixed context (edges of diffusion flames) and in a premixed context (edges of deflagrations), but the work reported here deals with the edges of diffusion flames. It is particularly relevant, we believe, to oscillations that have been seen in both the candle-flame context, and the flame-spread-over-liquid context. These oscillations are periodic edge-oscillations (in an appropriate reference frame), *sans* oscillation of the trailing diffusion flame.

References [4,5] examine a simple model of an anchored edge-flame, and construct solutions using DNS. It is shown that if the Lewis number of the fuel is sufficiently large (the Lewis number of the oxidizer is taken to be 1), and the Damköhler number is sufficiently small, oscillating-edge solutions can be found. Oscillations are encouraged by an on-edge convective flow and the insertion of a cold probe, discouraged by an off-edge convective flow.

In the present work, the nature of these oscillations is examined in more depth, using a variety of numerical strategies.

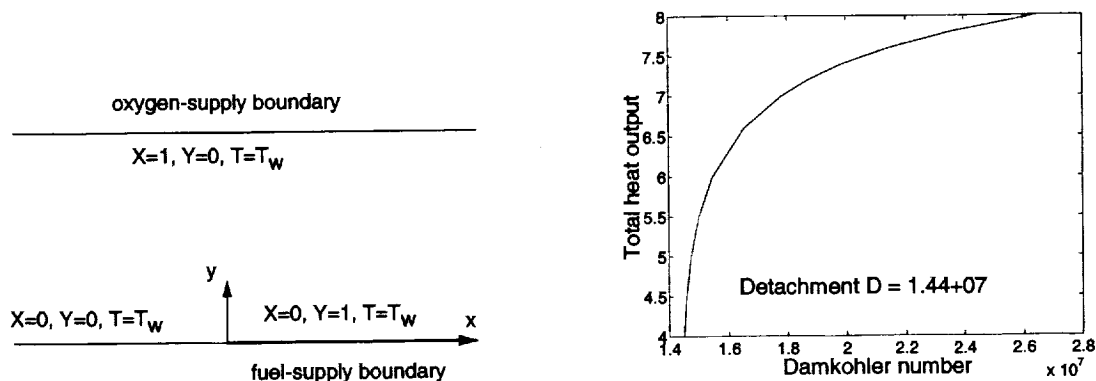


Figure 1: (i) The model configuration (the lower and upper boundaries are at $y = 0, y = 1$); (ii) Response diagram for the steady 2D solutions.

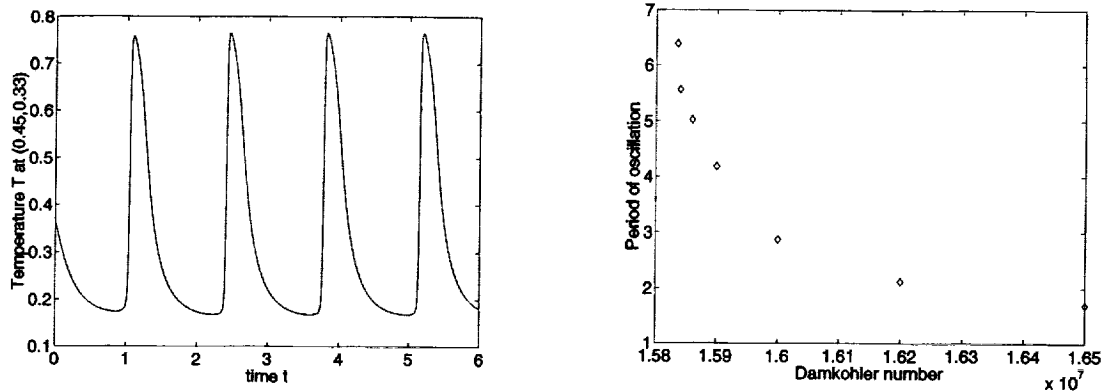


Figure 2: (i) Unstable solution for $D = 1.7 \times 10^7$; (ii) Variations of the period of oscillation with Damköhler number.

THE CONFIGURATION AND STEADY SOLUTIONS.

The model configuration, first introduced in [4], is sketched in Figure 1(i). The discontinuity in data at the fuel-supply boundary introduces a weak anchor for an edge-flame nominally located in the region $x > 0$. The field equations are

$$\frac{\partial}{\partial t} (T, X, Y) = \nabla^2 \left(T, \frac{1}{Le_X} X, \frac{1}{Le_Y} Y \right) + (q, -\alpha_X, -\alpha_Y) DXY e^{-\theta/T}, \quad (1)$$

and these describe a 1D frozen solution at $x \rightarrow -\infty$, a 1D diffusion flame solution at $x \rightarrow +\infty$. The latter is characterized by the familiar S-shaped response of diffusion flames, with an upper strong-burning branch when $D > D_{min}$. When

$$\alpha_X = \frac{1}{2}, \quad \alpha_Y = \frac{1}{2}, \quad Le_X = 1, \quad Le_Y = 2, \quad q = 1, \quad \theta = 6, \quad T_w = \frac{2}{13}$$

(values that we shall use throughout), we find $D_{min} = 0.79 \times 10^7$.

Solutions of the 2D problem defined by (1) are constructed using 4th-order spatial differencing and Runge-Kutta time integration. For some values of D , stationary solutions are unstable. To calculate these using the unsteady code we fix the integral

$$I_\Omega = \int_{x_{min}}^{x_{max}} dx \int_0^1 dy DXY e^{-\theta/T}. \quad (2)$$

Then at each fractional time step in the R-K integration in which X , Y , and T are adjusted, D is also adjusted to fix I_Ω . The solutions constructed in this way are characterized by the response of Figure 1(ii) where the total heat output (ordinate) is I_Ω , since here $q = 1$. This reveals a detachment Damköhler number, $D_{det} = 1.44 \times 10^7$, below which 2D solutions do not exist.

Unsteady DNS at fixed D identifies stable steady solutions at late time if $D > D_{ns}$, and oscillating solutions for some range of D in $D < D_{ns}$. Figure 2(i) shows temperature variations at a fixed point when $D = 1.7 \times 10^7$, a value less than D_{ns} ; indeed D_{ns} lies somewhere between 1.9273×10^7 and 1.9580×10^7 .

At this point we have identified three significant Damköhler numbers: the 1D quenching value $D_{min} = 0.79 \times 10^7$; the 2D stationary-edge detachment value $D_{det} = 1.44 \times 10^7$; and the 2D neutral stability value $D_{ns} \approx 1.94 \times 10^7$. A fourth significant number is the minimum value for

which oscillating (non-detached, non-quenched) solutions can be obtained. This is approximately $D = 1.583 \times 10^7$, a value greater than D_{det} . As $D \searrow 1.583 \times 10^7$, the amplitude of the oscillations increases, so that the maximum distance between the edge and the anchor point at $(0, 0)$ increases. Apparently both the amplitude and the period of the oscillations approach infinity, albeit slowly. Thus Figure 2(ii) shows the period for various D . The minimum D here is 1.5835×10^7 and x_{max} for the computational domain is 8, to prevent failure due to disappearance of the flame from the domain.

LINEAR STABILITY

We have seen how steady 2D edge-flame solutions can be constructed for all D greater than a critical detachment value, whether they are stable or unstable. These solutions can be used as the foundation of a linear stability analysis.

If we include z derivatives in the description (1) and linearize about the steady-state solution by writing

$$T = T_s + T', \quad \text{etc.}, \quad (3)$$

the perturbation variables satisfy the linear system

$$\frac{\partial}{\partial t} (X', Y', T') = \left(\frac{\partial^2}{\partial x^2} + \frac{\partial^2}{\partial y^2} - k^2 \right) \left(\frac{1}{Le_X} X', \frac{1}{Le_Y} Y', T' \right) + (-\alpha_X, -\alpha_Y, q) D [XY e^{-\theta/T}]', \quad (4)$$

where we have assumed that the perturbations are proportional to e^{ikz} , corresponding to corrugations in the z direction of specified wave-number. The boundary conditions are

$$T' = X' = Y' = 0 \quad \text{at } y = 0, 1; \quad \frac{\partial}{\partial x}(\cdot)' \rightarrow 0 \quad \text{as } |x| \rightarrow \infty. \quad (5)$$

For the parameter values examined here, the relevant 1D solution is stable for all D greater than the 1D quenching value.

A common strategy for discussing the solutions to systems such as (4), (5) is to make the replacement $\frac{\partial}{\partial t} \rightarrow \lambda$ and solve the eigenvalue problem by finite differencing and matrix methods. But an alternative is to use the unsteady solver that was used for all of the other numerical components of the problem. Time integration of (4), (5) with arbitrarily chosen initial conditions leads to an ever-growing solution if D lies to the left of D_{ns} . This growth can be monitored for one of the field variables, at a single point. Provided there is only a single unstable mode, both the growth rate $\mathcal{R}e(\lambda)$ and the frequency $\mathcal{I}m(\lambda)$ can be deduced from this output. At the same time, a late-time snapshot of the field variables identifies the eigenfunction, e.g. Figure 3(i). The dipole nature of the reaction-rate eigenfunction, Figure 3(i), is simply a reflection of the oscillating nature of the disturbance. When the reaction center, the core of the edge, moves to the left, the reaction rate is augmented at points on the left, diminished at points on the right, as here. Note that the perturbation is confined to the edge, and does not affect the trailing diffusion flame.

Figure 3(ii) shows variations in the growth rate $\mathcal{R}e(\lambda)$ with wave-number k when $D = 1.777 \times 10^7$. Variations of frequency with k are modest, and we do not show them. These results are typical of those that were found when D is in the unstable range. Further details and 3D DNS calculations that we have carried out will be reported elsewhere, but we note that the growth rate is a maximum when $k = 0$ and, consistent with this, the 3D DNS calculations show that 3D disturbances are suppressed in favor of 2D disturbances.

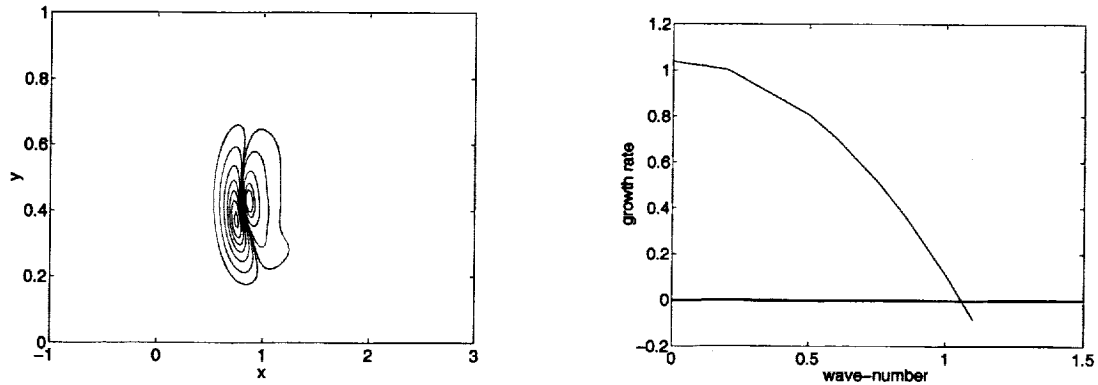


Figure 3: (i) Perturbation reaction-rate contours: the left group are positive, values 10 50 150 300 450 600 750; the right group are negative, values -10 -50 -150 -250 -300; (ii) Variations of growth rate with wave-number, $D = 1.777 \times 10^7$.

CONCLUDING REMARKS

In this study we have gained further insight into the nature of oscillating edge-flame solutions. But of greater interest, perhaps, is the demonstration that unsteady DNS can be used to construct unstable steady solutions and to solve the corresponding linear stability problem. The numerical examination of stability problems is commonplace in the fluid mechanics literature, but rare in the combustion literature, and perhaps the results presented here will encourage others to pursue this strategy in a variety of applications.

ACKNOWLEDGEMENTS

This work was supported by NASA-GLEN and by AFOSR.

REFERENCES

- [1] D.L.Dietrich, H.D.Ross, D.T.Frate, J.S.T'ien, Y.Shu, "Candle flames in microgravity", *Fourth International Microgravity Combustion Workshop*, NASA Conference Publication 10194 p.237 (1997).
- [2] H.D.Ross, F.J.Miller, "Flame spread across liquids", *Fifth International Microgravity Combustion Workshop*, NASA Conference Publication 1999-208917 p.321 (1999).
- [3] I.Kim, H.Li, W.A.Sirignano, "Flame spread across liquids: numerical modeling", *Fifth International Microgravity Combustion Workshop*, NASA Conference Publication 1999-208917 p.325 (1999).
- [4] J.Buckmaster and Yi Zhang, "A theory of oscillating edge-flames", *Combustion Theory and Modelling* **3** 547 (1999).
- [5] J.Buckmaster, A.Hegab, and T.L.Jackson, "More results on oscillating edge-flames", *Physics of Fluids* **12** 1592 (2000).